Ab Initio Studies on Nanoscale Friction between Graphite Layers: Effect of Model Size and Level of Theory

Raisa Neitola, Henna Ruuska, and Tapani A. Pakkanen*

Department of Chemistry, University of Joensuu, P.O. Box 111, FIN-80101 Joensuu, Finland

Received: December 31, 2004

Ab initio methods were used to investigate the nanoscale friction between two graphite layers placed in contact. The interaction energies were calculated for four two-layer models in series, $C_{6(n+1)^2}H_{6(n+1)}-C_{6n^2}H_{6n}$ with $n = 1$, 2, 3, and 4, and additionally for $C_{54}H_{18}-C_6H_6$ and $C_{150}H_{30}-C_6H_6$. The study was done with the Hartree−Fock method using basis sets 3-21G and 6-31G* and with the second-order Møller−Plesset theory using basis set 6-31G*. A density functional method (B3PW91) was also tested for reference purposes. The main interest was how the model size and level of theory affect the nanoscale friction coefficient. Most of the calculated friction coefficients fell within the range of values of 0.07−0.14.

1. Introduction

Graphite exhibits very low friction and wear on sliding on account of its layer−lattice structure, and it has the ability to form strong chemical bonds with gases. Because of these properties, graphite is one of the most widely used solid lubricants.[1−4] The low friction is widely exploited in sliding applications such as bearings and seals, while the unique mechanical and physical properties give it numerous industrial uses, in crucibles, moderators for nuclear reactors, heat exchangers, and electrodes. Graphitic materials and their applications are also of interest because of the resemblance, in structure and interactions, between graphite and carbon nanotubes. Nanotubes are promising a material for nanotechnological applications in energy storage, electronic devices, chemical sensors, and composite materials.[2,5−9] Understanding friction between graphite layers on the nanoscale is thus of wide importance.

Although friction is an everyday physical phenomenon, our understanding of the basic mechanism of nanoscale friction is insufficient. In recent years, development of new experimental techniques such as scanning probe microscopy, atomic force microscopy, friction force microscopy, and lateral force microscopy has enabled more specific insight into friction processes on the atomic scale.[1,10−12] These techniques are capable of measuring the force of friction between surfaces and examining lubrication at the interface between two solids, as well as producing images of interacting surfaces. Atomic force microscopy and friction force microscopy have been used to investigate the frictional properties and friction coefficient of hydrocarbon surfaces, including graphite and diamond.[13−22]

At the same time that progress in experimental techniques is providing a new dimension to the study of nanoscale friction, theoretical methods are offering a powerful tool to obtain information about the atomic-scale interactions and processes that cause friction. Several studies[7,23−33] on friction have demonstrated the applicability of molecular dynamics simulations and quantum chemical methods to describe the relationship between the microscopic and macroscopic phenomena of friction. Many groups have investigated atomic-scale friction, and also the coefficient of friction between layers of carbon materials (e.g., graphite, diamond, and nanotubes), by molecular dynamics simulations.[23−27] However, only a few quantum chemical studies[28−33] have focused on the mechanisms and interactions that cause friction on the nanoscale. The force of friction and the coefficient of friction have been calculated by ab initio methods for weakly interacting naphthalene and pyrene surfaces,[31] and we have evaluated the atomic-scale origin of friction between two different hydrocarbon layers.[32,33]

Because fundamental knowledge of nanoscale friction is essential for many technological applications, we undertook an investigation of the atomic-scale interactions between graphite layers by ab initio methods. Quantum chemical methods provide a powerful tool to examine the nature and consequences of the interactions between surfaces on the nanoscale. We chose the Hartree−Fock level of theory with basis sets 3-21G and 6-31G* since our previous studies showed that these are appropriate choices to model the friction between hydrocarbon layers. Furthermore, we tested the Møller−Plesset theory with the aim of evaluating its suitability for describing weak interactions, as well as the friction forces and coefficient of friction between graphite surfaces. In addition, reference calculations were performed with DFT methods. The interaction energies of the graphite models were calculated to obtain the friction coefficient between graphite surfaces on the nanoscale and to test for the appropriate model size and the level of theory.

2. Models and Computational Details

2.1. Models. Graphite models were constructed using information found in the literature:[1−4] the carbon atoms are arranged in a regular hexagonal structure (benzene rings), and the C−C bond length is 1.42 Å. Figure 1 presents the lamellar structure of hexagonal layered graphite with three staggered (ABA) layers. Five graphite monolayers of different sizes (C_6H_6, $C_{24}H_{12}$, $C_{54}H_{18}$, $C_{96}H_{24}$, $C_{150}H_{30}$) were used to investigate the friction between two graphite sheets. The monolayer models are shown in Figure 2. The models were terminated with hydrogen atoms, typical of covalent materials, to eliminate border effects. The C−H bond length was 1.072 Å, which was obtained from the optimization of benzene by the HF/3-21G method. The coordinates of the graphite layers were calculated so that the structure of the models conformed to D_{6h} symmetry. In all calculations the models were kept frozen; in other words, to maintain the

10.1021/jp044065q CCC: $30.25
Published on Web 05/04/2005

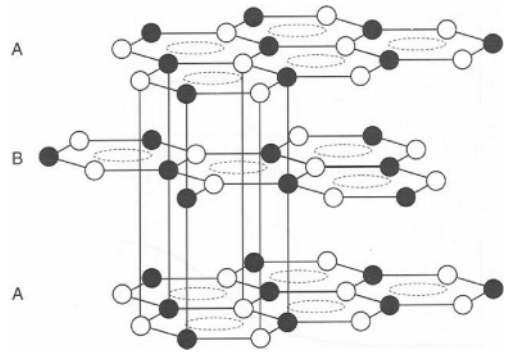

Figure 1. Hexagonal layered structure of graphite. Reprinted with permission from ref 1. Copyright 2002 John Wiley & Sons.

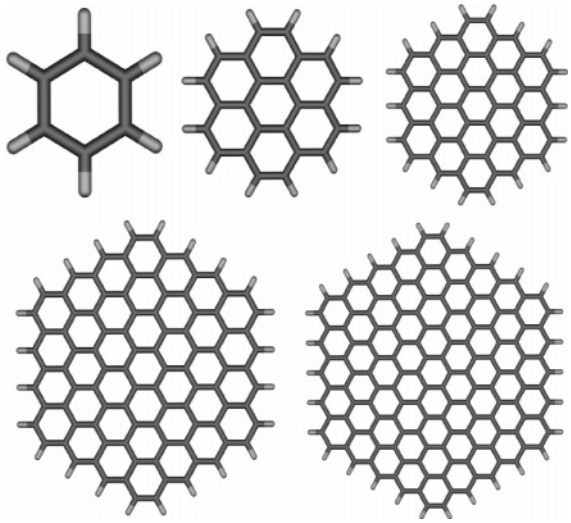

Figure 2. Graphite models viewed from the top. Dark gray hexagons represent carbon atoms and light gray hexagons hydrogen atoms.

symmetry, the graphite layers were not optimized. A monolayer model provides a good model of the graphite surface, since as a consequence of van der Waals forces the interactions between the basal planes are only weak and easily disrupted. As well, the diameters of our biggest models fit within the range of a realistic sheet of graphite crystallites (20−30 Å).[2,34] The diameter of $C_{96}H_{24}$ is almost 20 Å, and that of $C_{150}H_{30}$ is nearly 30 Å. The smallest monolayer models are stable organic compounds: benzene (C_6H_6), coronene ($C_{24}H_{12}$), and circumcoronene ($C_{54}H_{18}$).[34]

Investigation of the atomic-scale coefficient of friction requires calculations on two interacting layers. Thus, two one-layer models of different sizes placed against each other were used to calculate the interaction energies when two graphite layers slide against each other and then are pressed closer together. The two-layer models were chosen to be as large as possible while remaining computationally feasible. Figure 3 illustrates the two-layer models in the series $C_{6(n+1)^2}H_{6(n+1)}-C_{6n^2}H_{6n}$ with $n = 1$, 2, 3, and 4: that is, $C_{24}H_{12}-C_6H_6$, $C_{54}H_{18}-C_{24}H_{12}$, $C_{96}H_{24}-C_{54}H_{18}$, and $C_{150}H_{30}-C_{96}H_{24}$. Furthermore, outside the series, an interaction energy study was performed with models $C_{54}H_{18}-C_6H_6$ and $C_{150}H_{30}-C_6H_6$. The aim in investigating these models was to obtain a more exact picture of the effect of model size on the atomic-scale friction.

In calculating the friction coefficient by the technique described in previous investigations,[28−33] three different configurations were studied: eclipsed, $^1/_2$-staggered, and staggered. Examples of the three different configurations of the $C_{54}H_{18}-C_{24}H_{12}$ model are shown in Figure 4. In the eclipsed orientation,

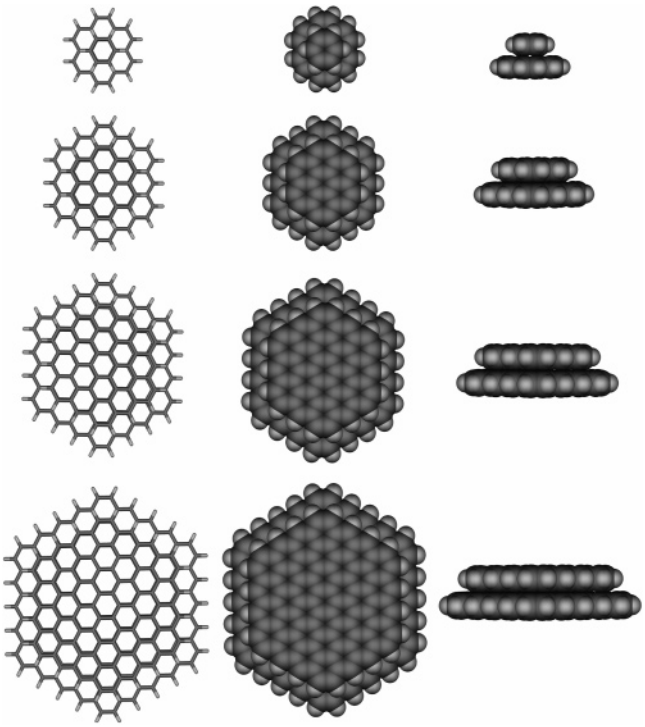

Figure 3. Two-layer models of graphite viewed from the side and the top as tube and space-fill forms, $C_{6(n+1)^2}H_{6(n+1)}-C_{6n^2}H_{6n}$ with $n = 1$, 2, 3, and 4. Dark gray spheres represent carbon atoms and light gray spheres hydrogen atoms.

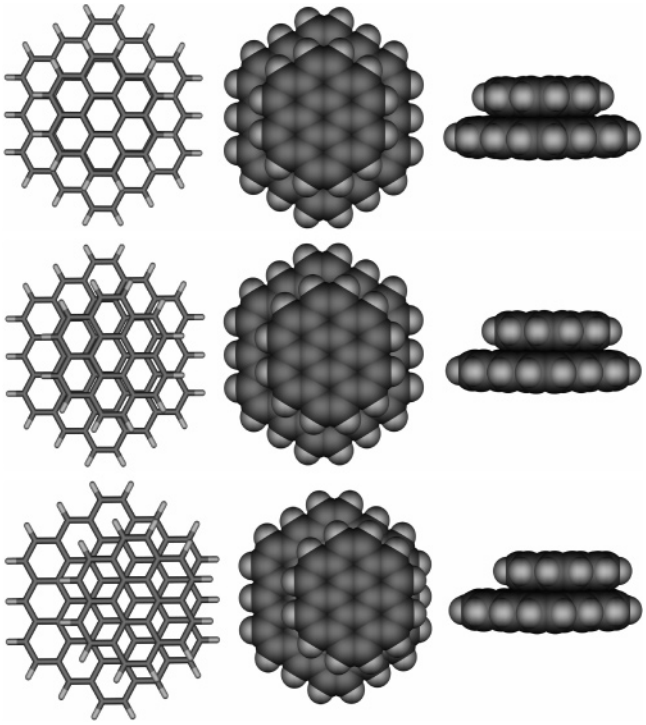

Figure 4. Graphite layers in interaction as viewed from the side for the $C_{54}H_{18}-C_{24}H_{12}$ model with a distance between the layers of 3 Å. Dark gray spheres represent carbon atoms and light gray spheres hydrogen atoms. The upper surface is successively moved to the right: (top) 0 Å (eclipsed configuration), (middle) 0.71 Å ($^1/_2$-staggered configuration), and (bottom) 1.42 Å (staggered configuration).

all carbon atoms of the upper sheet lie on top of the bottom carbons. In the $^1/_2$-staggered form, the upper layer has been moved 0.71 Å to the right so that none of the carbon atoms of the upper graphite sheet are situated on top of carbon atoms of

the lower sheet. In the staggered form, the upper layer has been moved 1.42 Å to the right and some of the carbon atoms of the upper sheet are situated above the center of the benzene rings of the underlying sheet. Only the eclipsed and staggered orientations were calculated for the biggest models ($C_{96}H_{24}-C_{54}H_{18}$ and $C_{150}H_{30}-C_{96}H_{24}$) to save computational resources.

2.2. Computational Details. In our previous friction studies on various hydrocarbon surfaces, the Hartree−Fock (HF) level of theory was found to produce reliable results for the friction coefficient.[32,33] In this work, therefore, calculations were mainly performed using the HF/3-21G and HF/6-31G* method and basis sets. The geometries and relative energies for equilibrium structures obtained with the HF method, at low computational expense, were often in good agreement with experimental values. HF theory fails, however, to adequately represent the electron correlation. The Møller−Plesset (MP) perturbation theory, in turn, is capable of describing the weak interaction energies between graphite sheets. To obtain improvement in the HF interaction energies, it was necessary, therefore, to use second-order Møller−Plesset (MP2) theory with basis set 6-31G*. Because the MP calculations are computationally intensive, only the two smallest models, $C_{24}H_{12}-C_6H_6$ and $C_{54}H_{18}-C_{24}H_{12}$, could feasibly be studied with the MP2/6-31G* level of theory. In particular, the basis set superposition error (BSSE) calculations with the MP method are demanding on computational resources because BSSE calculations ignore the symmetry of graphite layers. The capability of the density functional method B3PW91 to describe the interaction energy for eclipsed configurations of $C_{24}H_{12}-C_6H_6$ and $C_{54}H_{18}-C_{24}H_{12}$ models was also tested. BSSE was taken into account in all calculations, and it was eliminated by the counterpoise method.[35,36] The interaction energy, $\Delta E(r)$, of two graphite layers, A and B, at distance r was calculated as

$$\Delta E(r) = E^{AB}(r) - E^{A} - E^{B}$$

where the total energy of the double-layer system is $E^{AB}(r)$, and E^{A} and E^{B} are the energies of the separate graphite sheets. All energy calculations were performed with the Gaussian98 program package.[37]

3. Results and Discussion

3.1. Interaction Energies. We calculated the interaction energies for six two-layer graphite models of different sizes pressed closer together in small (0.1 Å) steps to obtain information about the microscale friction and the coefficient of friction. The distance between the carbon layers was varied between 3.0 and 2.0 Å. The interaction energy curves for graphite models in eclipsed and staggered configurations are plotted in Figures 5 and 6. Figures 5 and 6 depict only two stacking orientations since our investigations of two graphite layers in sliding contact showed the importance only of eclipsed and staggered configurations. These two configurations correspond to the points of maximum and minimum interaction energies in sliding contact. Sliding was modeled by moving the upper layer to the right in 16 steps so that the sliding was started in an eclipsed orientation and stopped in the next eclipsed orientation. The interaction energy increases as the distance between the graphite layers decreases, and likewise when the size of the graphite model is enlarged. This was not surprising since, in both cases, the repulsive interaction between graphite layers increased. To be more specific, as the layers were pressed closer together the repulsive interactions became stronger, and

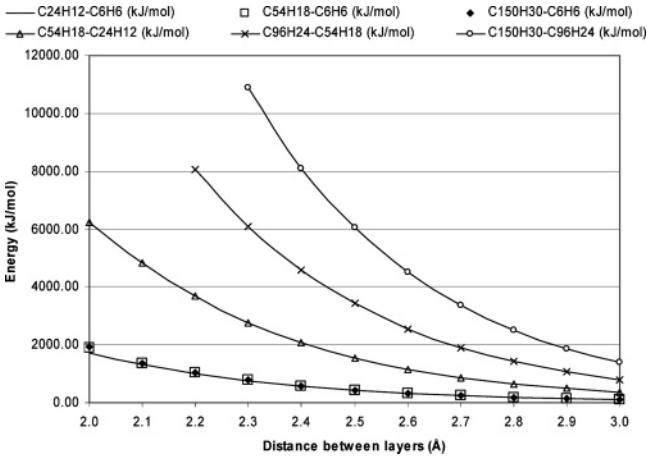

Figure 5. HF/3-21G interaction energies as a function of distance between the layers, shown for graphite models with the eclipsed configuration.

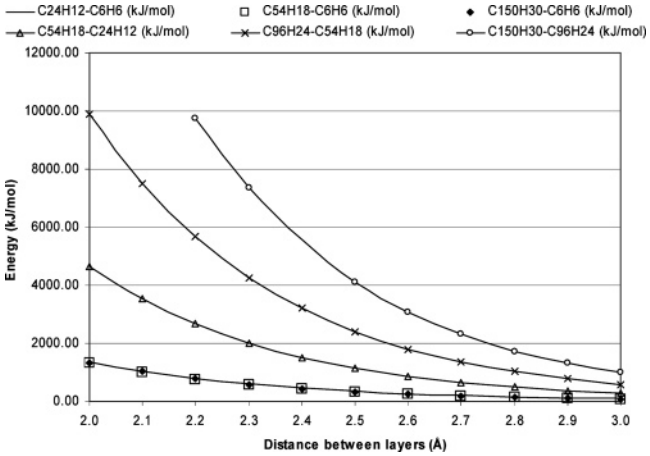

Figure 6. HF/3-21G interaction energies as a function of distance between the layers, shown for graphite models with the staggered configuration.

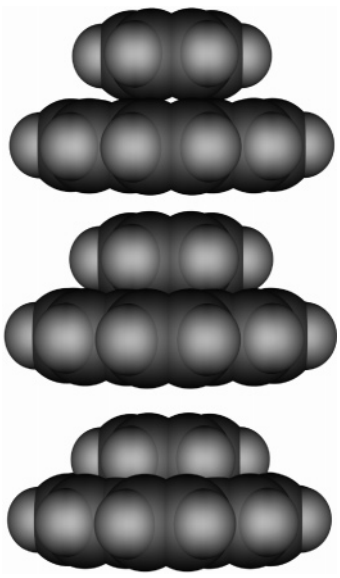

Figure 7. Graphite $C_{24}H_{12}-C_6H_6$ model under pressing. The distance between layers is (a) 3.0 Å, (b) 2.5 Å, and (c) 2.0 Å.

when the model size was larger, the number of contacting atoms increased. The visualization of the $C_{24}H_{12}-C_6H_6$ model with pressing (Figure 7) demonstrates the pressure caused by the repulsive forces between layers. When the distance was 3 Å,

TABLE 1: Interaction Energies per Carbon Atom *E* (kJ/mol) at Different Distances between Graphite Layers for the Eclipsed Configuration Calculated with the HF/3-21G Method

distance between graphite layers (Å)	$C_{24}H_{12}-C_6H_6$	$C_{54}H_{18}-C_6H_6$	$C_{150}H_{30}-C_6H_6$	$C_{54}H_{18}-C_{24}H_{12}$	$C_{96}H_{24}-C_{54}H_{18}$	$C_{150}H_{30}-C_{96}H_{24}$
3.0	17.61	17.32	17.06	15.33	14.70	14.44
2.9	22.95	22.90	22.63	20.31	19.61	19.33
2.8	30.16	30.42	30.14	27.06	26.26	25.96
2.7	39.86	40.57	40.24	36.18	35.26	34.92
2.6	52.90	54.22	53.82	48.46	47.37	46.96
2.5	70.38	72.53	72.01	64.90	63.54	63.00
2.4	93.69	96.98	96.28	86.76	84.94	84.16
2.3	124.62	129.51	128.49	115.56	112.95	113.49
2.2	165.39	172.55	171.01	153.06	149.05	
2.1	218.66	229.14	226.72	200.91		
2.0	287.39	317.37	320.34	259.31		

the layers barely touched one another, whereas at a distance of 2 Å the layers became "flattened" against each other.

The shape of the interaction energy curves for eclipsed configurations obtained with HF/3-21G was similar to the shapes for staggered orientations (see Figures 5 and 6). However, an examination of the series where only the size of the bottom layer changed ($C_{24}H_{12}-C_6H_6$, $C_{54}H_{18}-C_6H_6$, and $C_{150}H_{30}-C_6H_6$) shows the interaction energies to be essentially the same. In other words, the influence of a larger bottom layer on the interaction energies was inconsequential. The reason for this is that the contact area between the layers was the same in all three cases.

Comparison of the interaction energies in different stacking configurations of the graphite layers (Figures 5 and 6) shows the interaction energies for eclipsed models to be higher than those of staggered models. This is because interactions are more repulsive in the eclipsed orientation, where C atoms are lying on top of one other. The differences in interaction energy increase as the distance between the layers decreases and the size of the two-layer model increases. With the basis set 3-21G, the energies of the staggered configuration are about 15−30% smaller than the energies of the eclipsed configuration.

To obtain more information about the interaction between two graphite layers and the influence of the model size on the interaction energies, we examined the interaction energy per carbon atom. This was calculated by dividing the total interaction energy by the number of carbon atoms in the smaller layer of the model. The interaction energies per carbon atom are presented in Table 1. The energy values were more or less the same for all models in the eclipsed configuration and, separately, for all models in the staggered configurations. The energy values for the staggered configuration were about 2−50 kJ/mol lower than those for the eclipsed configuration, with the value depending on the distance between the graphite sheets. However, because of the small differences between the interaction energy values per carbon atom, the models roughly fall into two groups: $C_{24}H_{12}-C_6H_6$, $C_{54}H_{18}-C_6H_6$, $C_{150}H_{30}-C_6H_6$ and $C_{54}H_{18}-C_{24}H_{12}$, $C_{96}H_{24}-C_{54}H_{18}$, $C_{150}H_{30}-C_{96}H_{24}$. From the energy values, we can assume that it is unnecessary to enlarge the bottom layer to more than $n + 1$ ($C_{6(n+1)^2}H_{6(n+1)}-C_{6n^2}H_{6n}$). The $C_{54}H_{18}-C_{24}H_{12}$ model seems to be realistic and large enough to study the interaction between two graphite layers.

Besides studying the influence of model size on the interaction energies, we examined how different basis sets or methods affect the value of the interaction between two graphite sheets. Because the ab initio calculations at this level of theory are time-consuming, we concentrated on just two models, $C_{24}H_{12}-C_6H_6$ and $C_{54}H_{18}-C_{24}H_{12}$, calculated with the HF/3-21G, HF/6-31G*, B3PW91/6-31G*, and MP2/6-31G* levels of theory. The interaction energies with the different levels of theory for eclipsed and staggered situations are presented in Figures 8 and 9. Interaction energies calculated with HF/3-21G were almost identical with those calculated with the HF/6-31G* method. As expected, however, the differences in the interaction energies between HF and the correlated MP2 method were considerable: interaction energies with the MP2 method were much lower that those with the HF method. The relative difference in interaction energy values was most pronounced for the $C_{54}H_{18}-C_{24}H_{12}$ model. DFT interaction energies for eclipsed configurations are between the HF and MP2 energies. At small distances (<2.5 Å), the B3PW91 interaction energies approach the MP2 results. The differences between the DFT and MP2

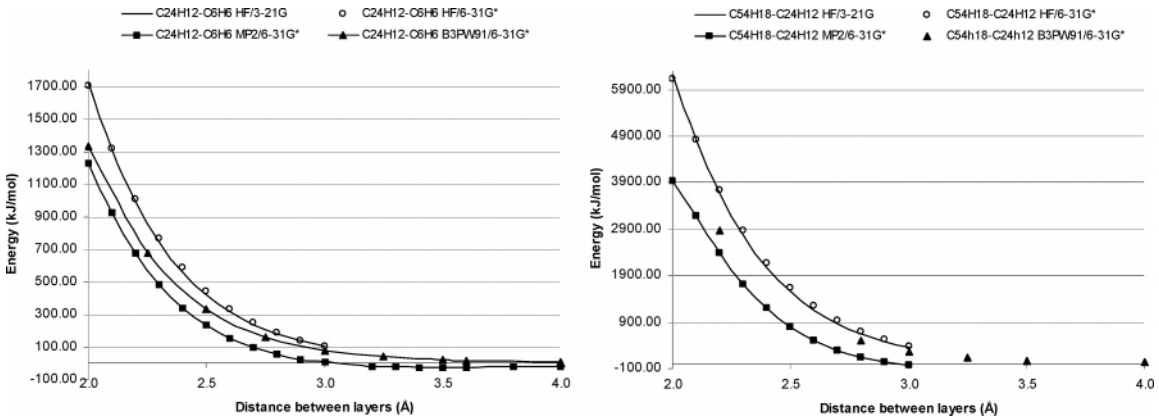

Figure 8. Comparison of interaction energies *E* (kJ/mol) for eclipsed $C_{24}H_{12}-C_6H_6$ and $C_{54}H_{18}-C_{24}H_{12}$ models calculated at the HF/3-21G, HF/6-31G*, B3PW91/6-31G*, and MP2/6-31* levels of theory.

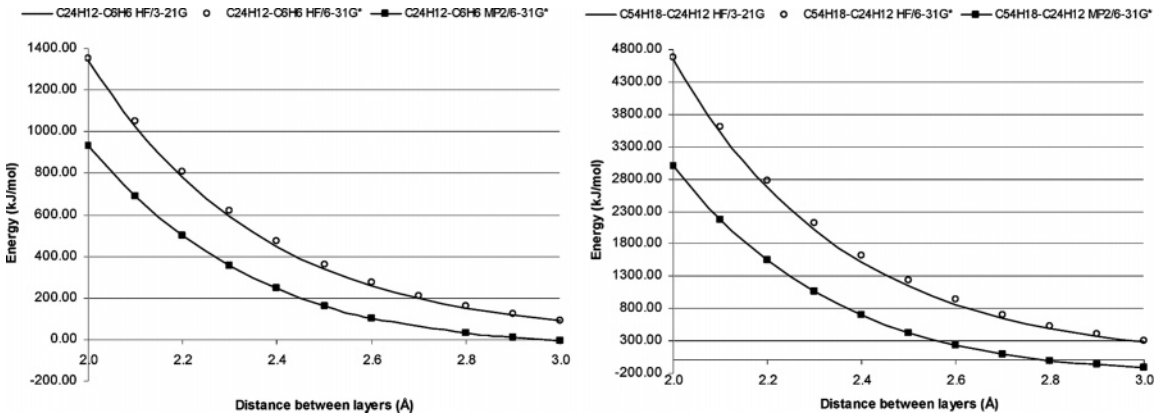

Figure 9. Comparison of interaction energies E (kJ/mol) for staggered $C_{24}H_{12}-C_6H_6$ and $C_{54}H_{18}-C_{24}H_{12}$ models calculated at the HF/3-21G, HF/6-31G*, B3PW91/6-31G*, and MP2/6-31* levels of theory.

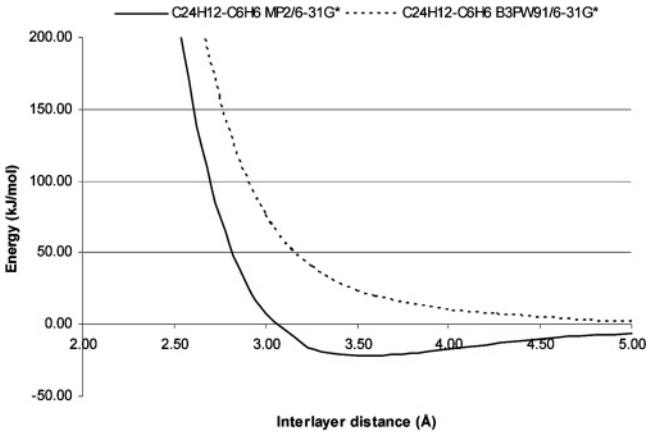

Figure 10. MP2/6-31G* and B3PW91 interaction energy curves as a function of interlayer distance for the eclipsed $C_{24}H_{12}-C_6H_6$ model.

methods are more significant at large interlayer distances (2.5−5.0 Å): the B3PW91/6-31G* interaction remains repulsive, while the MP2 method shows a minimum with an interaction energy of −22 kJ/mol as shown in Figure 10. At the HF and DFT levels the interaction energies were repulsive in both models, at all distances, but at the MP2 level the interaction energies became attractive at the largest distance. Only the repulsive interaction is of interest for an examination of friction forces and the coefficient of friction between graphite layers.

3.2. Coefficient of Friction. Examination of the coefficient of friction was the final goal of our atomic-scale friction studies. The interaction energies of the graphite models summarized above are needed to calculate the force of friction and the coefficient of friction by the procedure of Zhong and co-workers.[28−31] First, a polynomial function was fitted to the curve of the interaction energy (Figures 5 and 6), and the function was differentiated to obtain the normal load, F_N. The friction force on the atomic scale under normal load was then obtained by calculating the energy difference between the eclipsed and staggered configurations (minimum and maximum) and dividing this by the difference in distance between the minimum and maximum values. The coefficient of friction is the friction force divided by the normal load.

Our calculated coefficients of friction fall within the range of values of 0.05−0.16 at a normal load of 10−200 nN. Table 2 shows that the coefficient of friction was typically about 0.07. The deviations from this value were greatest for the two smallest graphite models, $C_{24}H_{12}-C_6H_6$ and $C_{54}H_{18}-C_{24}H_{12}$, at the levels HF/3-21G and HF/6-31G*. The coefficient of friction was clearly highest for the $C_{24}H_{12}-C_6H_6$ model, probably as a consequence of the inadequate size of the model. Noteworthy was that the values calculated at the HF/3-21G and HF/6-31G* levels were almost the same. Accordingly, the bigger models ($C_{96}H_{24}-C_{54}H_{18}$, $C_{150}H_{30}-C_{96}H_{24}$) were calculated only with the 3-21G basis set. For these models the value of the friction coefficient does not deviate much from 0.07, even though the range of normal load was greater for the $C_{150}H_{30}-C_{96}H_{24}$ model than the other model. The coefficient of friction with MP2/6-31G* was examined only for the smallest ($C_{24}H_{12}-C_6H_6$) model, both because the MP2 method is very time-consuming and because the interaction energies became attractive for the $C_{54}H_{18}-C_{24}H_{12}$ model (see Figure 9). Table 3 presents the average coefficient of friction for graphite models at different levels of theory. The coefficient of friction obtained for the $C_{24}H_{12}-C_6H_6$ model with the MP2 method agrees well with the coefficient obtained with bigger models with the HF method. Extrapolating from Table 3, the friction coefficient for the biggest model with MP2 could be supposed to be as low as 0.03−0.05.

Direct comparisons of our calculated atomic-scale coefficient of friction with experimental coefficients for graphite are not easily made because there is no unambiguous value of the coefficient of friction. In fact, the coefficient of friction depends on many factors. The effects of surface structure and roughness and the environment of sliding and normal load, for example, give rise to a large number of different coefficient values. An ultrasmall atomic-scale coefficient of friction (0.006−0.012) has been measured for highly oriented pyrolytic graphite.[14,18,38] A similarly low frictional coefficient for graphite (0.011−0.015) has been found in some theoretical investigations[23,31] on the atomic scale. For instance, Matsuzawa and Kishii[31] obtained a low coefficient of friction for the naphthalene/hydrogen system with the MP2 method. According to other experimental studies, however, the coefficient of friction may be about an order of magnitude larger than the ultrasmall coefficient of friction, varying with the gaseous composition of the environment.[39−46] In the presence of molecular oxygen the coefficient of friction ranges between 0.2 and 0.45 due to the pressure.[41] Moreover, the coefficient of friction is typically 10 times as great in a vacuum or dry nitrogen as in air.[1] A typical macroscopic coefficient of friction of graphite is about 0.1.[1,31] Our calculated coefficient of friction (0.05−0.16) is in agreement with this value as well as with many atomic-scale values. In addition, our value is of the same order of magnitude as the coefficient of friction measured for graphite in a vacuum (0.15) and calculated by molecular dynamics (0.099).[23,47]

TABLE 2: Calculated Coefficient of Friction for Graphite Models

normal load (nN)	$C_{24}H_{12}-C_6H_6$			$C_{54}H_{18}-C_{24}H_{12}$		$C_{96}H_{24}-C_{54}H_{18}$	$C_{150}H_{30}-C_{96}H_{24}$
	HF/3-21G	HF/6-31G*	MP2/6-31G*	HF/3-21G	HF/6-31G*	HF/3-21G	HF/3-21G
10.0	0.15	0.16	0.06				
15.0	0.14	0.15	0.07				
20.0	0.13	0.14	0.07	0.11	0.08		
25.0	0.13	0.14	0.07	0.09			
30.0	0.12	0.14	0.08	0.08	0.10		
40.0	0.12	0.14	0.07	0.08	0.10		
50.0	0.12	0.14	0.06	0.09	0.11	0.07	
60.0				0.09	0.11	0.07	
70.0				0.08	0.10	0.07	
80.0				0.08	0.10	0.07	
90.0				0.07	0.09	0.07	
100.0				0.07	0.09	0.07	
110.0							
120.0							0.06
130.0							0.07
140.0							0.08
150.0						0.06	0.08
160.0							0.08
170.0							0.07
180.0							0.07
190.0							0.06
200.0						0.05	0.05

TABLE 3: Average of the Calculated Coefficients of Friction for Graphite Models

model	HF/3-21G	HF/6-31G*	MP2/6-31G*
$C_{24}H_{12}-C_6H_6$	0.13	0.14	0.07
$C_{54}H_{18}-C_{24}H_{12}$	0.08	0.10	
$C_{96}H_{24}-C_{54}H_{18}$	0.07		
$C_{150}H_{30}-C_{96}H_{24}$	0.07		

4. Conclusions

We calculated the interaction properties of four two-layer graphite models ($C_{6(n+1)^2}H_{6(n+1)}-C_{6n^2}H_{6n}$ with $n = 1$, 2, 3, and 4) with the aim of finding a suitable model size and level of theory for nanoscale friction studies. Our calculations of graphite surfaces provide atomic-scale information about the interaction energies between two weakly interacting surfaces as well as the coefficient of friction. Although our previous studies suggested that HF methods are appropriate for modeling the friction properties of hydrocarbon layers, in this study we also tested the DFT and MP2 levels of theory.

Our calculations of graphite layers showed that interaction energies were highest when the repulsive forces were strongest, in other words, when the graphite layers were eclipsed and the distance between layers was increased to 2.0 Å. In addition, the number of repulsive interactions between the surfaces increased with the size of the model. The differences in the results with the HF/3-21G and HF/6-31G* methods were almost negligible. As expected, the interaction energies obtained with the MP2/6-31G* method were lower than the corresponding values obtained with the HF method, and the B3PW91 interaction energies are between the HF and MP2 interaction energy values. Furthermore, with the MP2/6-31G* method, the interaction energies for the $C_{54}H_{18}-C_{24}H_{12}$ model became attractive when the layers were furthest apart. Attractive forces are not appropriate for an examination of the coefficient of friction.

The calculated coefficient of friction for graphite surfaces ranged from 0.05 to 0.16 at a normal load of 10−200 nN, which is in agreement with other investigations of the friction coefficient. Comparison of the friction coefficient calculated with different levels of theory showed that the $C_{54}H_{18}-C_{24}H_{12}$ model is large enough for friction studies with HF methods, but even the smallest model can be used for friction calculations with the MP2 method. Although our computational resources were inadequate for MP2 calculations of bigger models, we presume that, with larger models, the coefficient of friction for graphite surfaces would be something like 0.03−0.05. The graphite models used in this study for research on nanoscale friction can also serve as models for describing the friction properties of multiwalled nanotubes.

References and Notes

(1) Bhushan, B. *Introduction to Tribology*; John Wiley & Sons: New York, 2002.
(2) Patric, J. W. *Porosity in Carbons*; Edward Arnold: London, 1995.
(3) Borg, R. J.; Dienes, G. J. *The Physical Chemistry of Solids*; Academic Press: San Diego, 1992.
(4) Jakubke, H.-D.; Jeschkeit, H. *Concise Encyclopedia Chemistry*; Walter de Gruyter & Co.: Berlin, 1993.
(5) Johnston, R. L. *Atomic and Molecular Clusters*; Taylor & Francis: London, 2002.
(6) Dai, H. *Surf. Sci.* **2002**, *500*, 218.
(7) Buldum, A.; Lu, J. P. *Appl. Surf. Sci.* **2003**, *219*, 123.
(8) Miura, K.; Takagi, T.; Kamiya, S.; Sahashi, T.; Yamauchi, M. *Nano Lett.* **2001**, *1*, 161.
(9) Cumings, J.; Zettl, A. *Science* **2000**, *289*, 602.
(10) Bhushan, B. *Modern Tribology Handbook I−II*; CRC Press: Boca Raton, FL, 2001.
(11) Bhushan, B. *Handbook of Micro/Nanotribology*, 2nd ed.; CRC Press: Boca Raton, FL, 1999.
(12) Bhushan, B. *Fundamentals of Tribology and Bridging the Gap Between the Macro- and Micro/Nanoscales*; Kluwer Academic Publishers: Dordrecht, The Netherlands, 2001.
(13) Ruan, J.-A.; Bhushan, B. *J. Appl. Phys.* **1994**, *76*, 5022.
(14) Ruan, J.-A.; Bhushan, B. *J. Appl. Phys.* **1994**, *76*, 8117.
(15) Liu, D. P.; Benstetter, G.; Frammelsberger, W. *Appl. Phys. Lett.* **2003**, *82*, 3898.
(16) Liu, D.; Benstetter, G.; Liu, Y. H.; Zhang, J. L.; Ren, C. S.; Ma, T. C. *Surf. Coat. Technol.* **2003**, *174−175*, 310.
(17) Liu, D.; Benstetter, G.; Lodermeier, E.; Akula, I.; Dudarchyk, I.; Liu, Y.; Ma, T. *Surf. Coat. Technol.* **2003**, *172*, 194.
(18) Mate, C. M.; McClelland, G. M.; Erlandsson, R.; Chiang, S. *Phys. Rev. Lett.* **1987**, *59*, 1942.
(19) Liu, E.; Blanpain, B.; Celis, J. P. *Wear* **1996**, *192*, 141.
(20) Schwarz, U. D.; Zwörner, O.; Köster, P.; Wiesendanger, R. *Phys. Rev. B* **1997**, *56*, 6987.
(21) Sasaki, N.; Kobayashi, K.; Tsukada, M. *Phys. Rev. B* **1996**, *54*, 2138.
(22) Sasaki, N.; Kobayashi, K.; Tsukada, M. *Surf. Sci.* **1996**, *357−358*, 92.
(23) Matsushita, K.; Matsukawa, H.; Sasaki, N. *Condens. Matter* **2003**, 1−12.
(24) Ni, B.; Sinnott, S. B. *Surf. Sci.* **2001**, *487*, 87.

(25) Ni, B.; Sinnott, S. B.; Mikulski, P. T.; Harrison, J. A. *Phys. Rev. Lett.* **2002**, *88*, 205505−1.
(26) Servantie, J.; Gaspard, P. *Phys. Rev. Lett.* **2003**, *91*, 185503−1.
(27) Harrison, J. A.; Perry, S. S. *MRS Bull.* **1998**, *23*, 27 and references therein.
(28) Zhong, W.; Tománek, D. *Phys. Rev. Lett.* **1990**, *64*, 3054.
(29) Tománek, D.; Zhong, W.; Thomas, H. *Europhys. Lett.* **1991**, *8*, 887.
(30) Overney, G.; Zhong, W.; Tománek, D. *J. Vac. Sci. Technol., B* **1991**, *9*, 479.
(31) Matsuzawa, N. N.; Kishii, N. *J. Phys. Chem. A* **1997**, *101*, 10045.
(32) Neitola, R.; Pakkanen, T. A. *J. Phys. Chem. B* **2001**, *105*, 1338.
(33) Neitola, R.; Pakkanen, T. A. *Chem. Phys.* **2004**, *299*, 47.
(34) Ruuska, H.; Pakkanen, T. A. *J. Phys. Chem. B* **2001**, *105*, 9541.
(35) Scheiner, S. *Molecular Interactions*; John Wiley & Sons: New York, 1997.
(36) Kestner, N.; Combariza, J. In *Reviews in Computational Chemistry*; Lipkowitz, K. B., Boyd, D. B., Eds.; John Wiley & Sons: New York, 1999.
(37) Frisch, M. J.; Trucks, G. W.; Schlegel H. B.; et al. *Gaussian 98*, Revision A.7; Gaussian, Inc.: Pittsburgh, PA, 1998.
(38) Mate, C. *Wear* **1993**, *168*, 17.
(39) Xiaowei, L.; Suyuan, Y.; Xuanyu, S.; Shuyan, H. *Sci. China* **2001**, *44*, 248.
(40) Csapo, E.; Zaidi, H.; Paulmier, D. *Wear* **1996**, *192*, 151.
(41) Zaidi, H.; Csapo, E.; Nery, H.; Paulmier, D.; Mathia, T. *Surf. Coat. Technol.* **1993**, *62*, 388.
(42) Zaidi, H.; Robert, F.; Paulmier, D.; Nery, H. *Appl. Surf. Sci.* **1993**, *70/71*, 103.
(43) Zaidi, H.; Mezin, A.; Nivoit, M.; Lepage, J. *Appl. Surf. Sci.* **1989**, *40*, 103.
(44) Paulmier, D.; Zaidi, H. *Vacuum* **1990**, *41*, 1314.
(45) Zaidi, H.; Paulmier, D.; Lepage, J. *Appl. Surf. Sci.* **1990**, *44*, 221.
(46) Haltner, A. J. *ASLE Trans.* **1966**, *9*, 136.
(47) Zaidi, H.; Paulmier, D.; Jeanmaire, A.; Nery, H. *Surf. Sci.* **1991**, *251/252*, 778.